ISSN 0029 - 3865

CBPF-NF-025/88

GAP ROAD: A NEW PATH TO CHAOS*

by

M.C. de Sousa VIEIRA and C. TSALLIS

Centro Brasileiro de Pesquisas Físicas - CBPF/CNPq
Rua Dr. Xavier Sigaud, 150
22290 - Rio de Janeiro, RJ

*To appear in "Disordered Systems in Biological Models", eds. L. Peliti and S.A. Solla (World Scientific, 1988).

ABSTRACT

We study numerically the asymmetric map $x'=1-\varepsilon_i-a_i|x|^{z_i}$ ($i=1,2$ respectively, correspond to $x>0$ and $x\leq 0$). The standard logistic-like equation is recovered for $a_1=a_2$, $z_1=z_2=2$ and $\varepsilon_1=\varepsilon_2=0$. Three types of asymmetry are studied, namely those concerning the amplitude ($a_1\neq a_2$), the exponent ($z_1\neq z_2$) and a possible discontinuity ($\varepsilon_1\neq\varepsilon_2$). The well known period-doubling road to chaos is topologically unmodified in the two first cases, but in the last one the scenario is completely new ("gap road to chaos"). Chaos is now attained through sequences of inverse cascades. Various new features are observed concerning the phase-diagrams, Liapunov and uncertainty exponent, number of attractors, multifractality, among others.

Key-words: Population dynamics; Chaos; Dynamical Systems.

1. INTRODUCTION

Chaotic evolution of a dynamical system is a field that aroused a great interest in the last decade. May[1], in 1976, showed the rich behavior that a nonlinear finite-differences equation can present, through a simple model for the population dynamics.In the model the death rate of a given biological population x_{t+1}, in generation t+1, is assumed to vary linearly with the population x_t (associated with generation t). Such dynamics are described by the logistic equation, $x_{t+1} \propto x_t(1-x_t)$ which, through a trivial changement of variables, can be rewritten a follows

$$x_{t+1} = f(x_t) \equiv 1-ax_t^2 \qquad (1)$$

where the interesting behavior appears for $x \in [-1,1]$ and $a \in [0,2]$: See Fig. 1(a). This equation, in spite of its simplicity, displays a surprisingly rich mathematical structure. For certain values of the control parameter a, the long-time sequence $\{x_t\}$ is a cycle, and for others it is chaotic. There exists many situations, others than in population Biology,where the logistic equation applies. For example, in Genetics, Epidemiology, Economics, etc. In Physics, it appears in many branches, such as fluid mechanics[2], chemical systems[3], laser physics[4] and others.

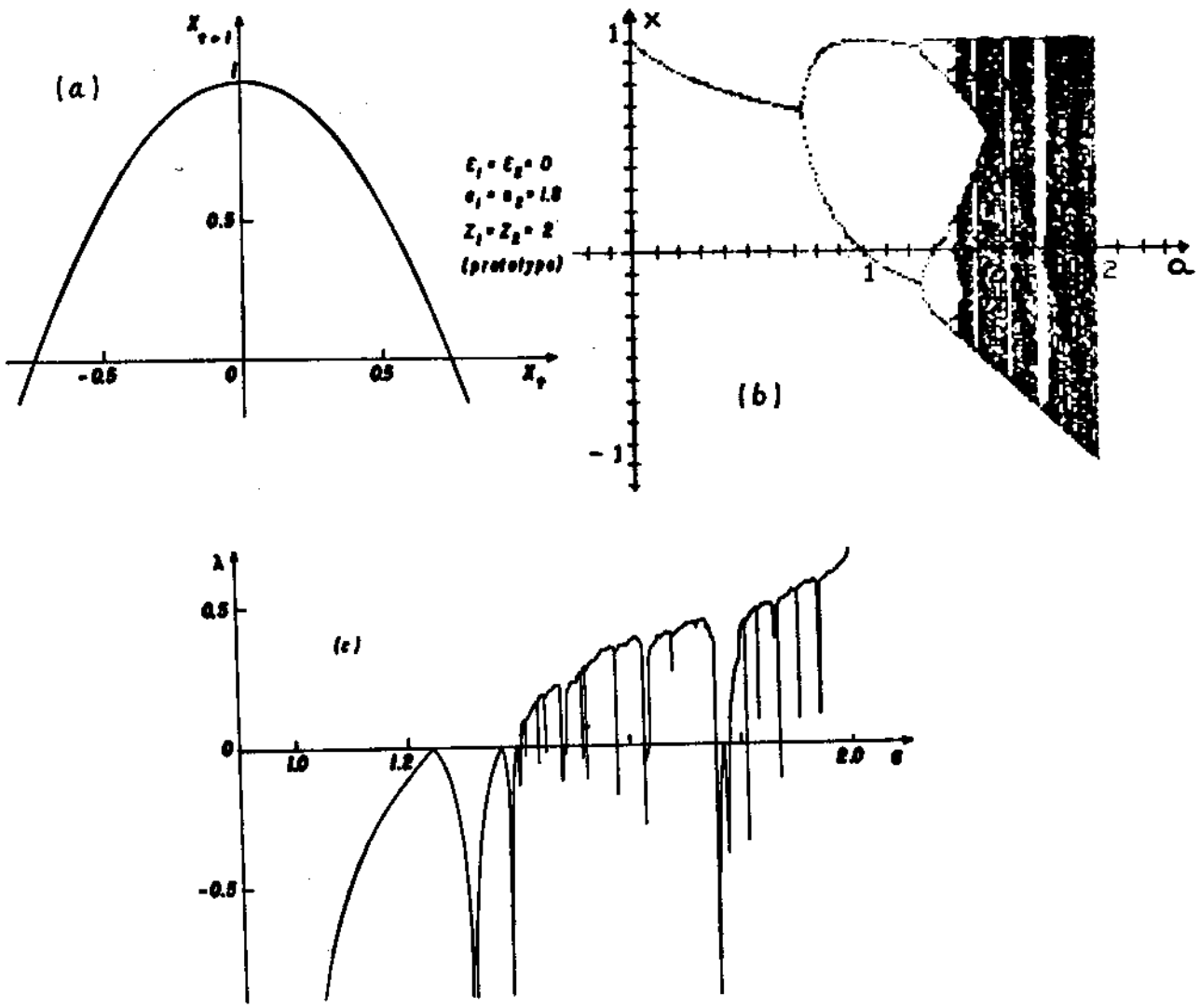

Fig. 1. (a) Logistic map, (b) a-evolution of the attractor and of the (c) Liapunov exponent.

A fixed point x* of the mapping is defined by $x^*=f(x^*)$. Such a point is said to be stable, unstable or "marginally" stable, if $|f'(x^*)|$ is less, greater or igual to the unit, respectively. For the logistic map, for $a<a_1=0.75$, there is only one stable point. Just above the value a_1 this point becomes unstable and there appears instead a new attractor, namely a cycle of period two. This process is called *pitchfork bifurcation*. The cycle remains stable until a increases up to $a_2=1.25$, where another bifurcation appears and we have now a four-cycle. This bifurcation process will continue until $a^*=1.401155...$ is reached. Above a* we see the chaotic regime, where odd cycles and aperiodic attractors are present, as well. The behavior of the attractor as function of a is depicted in Fig. 1(b).

As shown by Grossmann and Thomae, by Feigenbaum and by Coullet and Tresser[5], the sequence $\{a_k\}$ where bifurcations occur, converges geometrically at a rate given by

$$\delta_k \equiv \frac{a_k - a_{k-1}}{a_{k+1} - a_k} \to \delta = 4.6692... \qquad (2)$$

for large values of k. This is an universal exponent, in the sense that it depends only on the quadratic shape of f(x) at the extremum.

In the chaotic zone there are infinite periodic windows, with period doubling bifurcations governed by (2). Metropolis, Stein and Stein[6] discovered a universal behavior in the sequence of these windows for single hump one-dimensional maps.

The chaotic regime is characterized by a high sensitivity on the initial conditions (value of x_0). The Liapunov exponent λ provides a quantitative measure of this dependence ($\lambda<0$ corresponds to periodic orbits, and $\lambda>0$ corresponds to chaotic motion; λ vanishes on every pitchfork bifurcation). The Liapunov exponent is defined through

$$\lambda \equiv \lim_{N\to\infty} \frac{1}{N} \sum_{t=0}^{N-1} \ln \left| \frac{df(x)}{dx} \right|_{x=x_t} \qquad (3)$$

In Fig. 1(c) we display λ as a function of a for the map governed by (1). In the chaotic region we can see intervals with negative λ exponent, corresponding to the periodic windows.The largest of them is the period three window.

The aim of the present paper is to study the dynamical behavior of a map with an asymmetry introduced at the extremum. Until now, little effort has been dedicated to asymmetric maps[7-12]. Experimental systems are now appearing which present this type of dynamics (see [11] for laser cavity and [12] for forced nonlinear oscillators), and therefore the study of such maps becomes increasingly relevant.

We will generalize the logistic map as follows:

$$x_{t+1} = f(x_t) \equiv \begin{cases} 1-\varepsilon_1-a_1|x_t|^{z_1} & \text{if } x>0 \\ 1-\varepsilon_2-a_2|x_t|^{z_2} & \text{if } x\leq 0 \end{cases} \qquad (4)$$

The well known continuous symmetric case ($\varepsilon_1=\varepsilon_2=0$, $a_1=a_2\equiv a$ and $z_1=z_2\equiv z$) presents the same qualitative behavior of the $z=2$ case (logistic equation). The convergence rates of the δ's in these maps, are a monotonously increasing function of $z\geq 1$ [13].

For sake of simplicity, we shall proceed by modifying one type of parameter (the a's, the z's and the ε's) at a time. We shall therefore consider three cases, namely, case I ($a_1\neq a_2$, $z_1=z_2\equiv z$ and $\varepsilon_1=\varepsilon_2=0$), case II ($a_1=a_2\equiv a$, $z_1\neq z_2$ and $\varepsilon_1=\varepsilon_2=0$), and case III ($a_1=a_2\equiv a$, $z_1=z_2\equiv z$ and $\varepsilon_1\neq\varepsilon_2$). Some features of these maps, such as phase-diagrams, attractors, Liapunov exponents, uncertainty exponent, multifractality, and others will be studied in the following sections.

2. AMPLITUDE ASYMMETRY (CASE I)

In this case , the scenario of pitchfork bifurcations is preserved. Nevertheless, the set $\{\delta_k\}$ presents an oscillatory behavior between *two* fixed values[7]. Let us now mention at

this point that preliminary numerical work[10] suggested that δ_k approaches a single value, namely that of the symmetric case. The present high accuracy calculations show that this is not so, but rather exhibit the oscillatory behavior first studied by Arneodo et al[7]. We have represented in Fig. 2(a) for $z_1=z_2=2$ and $\varepsilon_1=\varepsilon_2=0$, the (a_1,a_2) critical lines which generalize a^* (first entrance into chaos) and a^M (value of a above which attractors disappear). In Fig. 2(b) we show, for k large enough, the oscillatory behavior of the set $\{\delta_k\}$ as function of a_2^* over the curve a_2^* of Fig. 2(a). Observe that in $a \cong 1.401155$, $a_1^*=a_2^*$, therefore the two values of δ_k coincide, and reproduce the well known value 4.6692... .

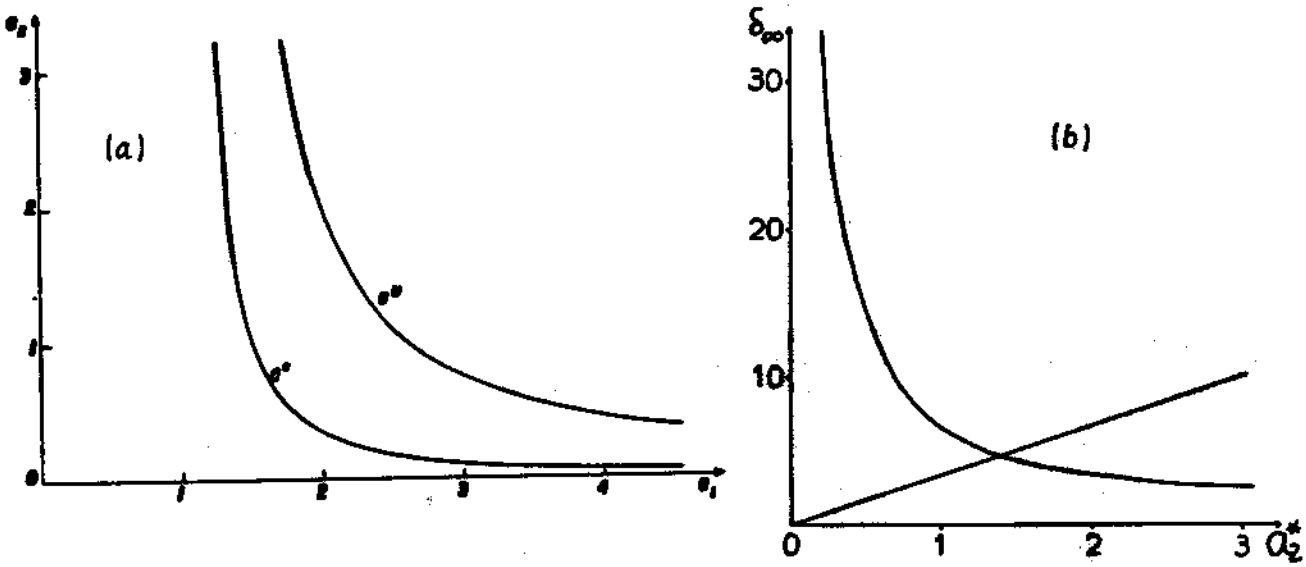

Fig. 2. (a) Special cuts of the "first entrance into chaos" and "finite-attractor-disappearance" hypersurfaces in the a_1,a_2 space for $z_1=z_2=2$ and $\varepsilon_1=\varepsilon_2=0$, (b) values of δ_k, for $k\gg1$ as function of a_2^*, calculated over the line a_2^* of (a). The numerical results for the asymptotic values are roughly reproduced by $\delta_\infty \cong 3.3a_2^*$ and $\delta_\infty \cong 7/a_2^*$.

3. EXPONENT ASYMMETRY (CASE II)

In this case the route to chaos is via period-doubling. In Fig.3 we have represented the a-dependence of the attractor and of λ for a typical case, namely $(z_1,z_2)=(2,4)$. The accumulation point of the first period-doubling cascade is $a^*\cong 1.6414$ and $a^M=2$. A strongly different behavior appears as already noticed[9], in the set $\{\delta_k\}$: the δ_k's do not converge for increasing k, but proceed in oscillatory fashion between two asymptotic lines, one of them being divergent. In Fig. 4 we have presented our results as well as the numerical ones obtained in Ref. 9. This behavior was also exhibited experimentally[12]. Above a* (chaotic region), the relative sizes of the various windows are quite different from those of the $z_1=z_2$ prototype. However the sequence of high-order windows is the same of the symmetric case, since this map satisfy the conditions required in [6].

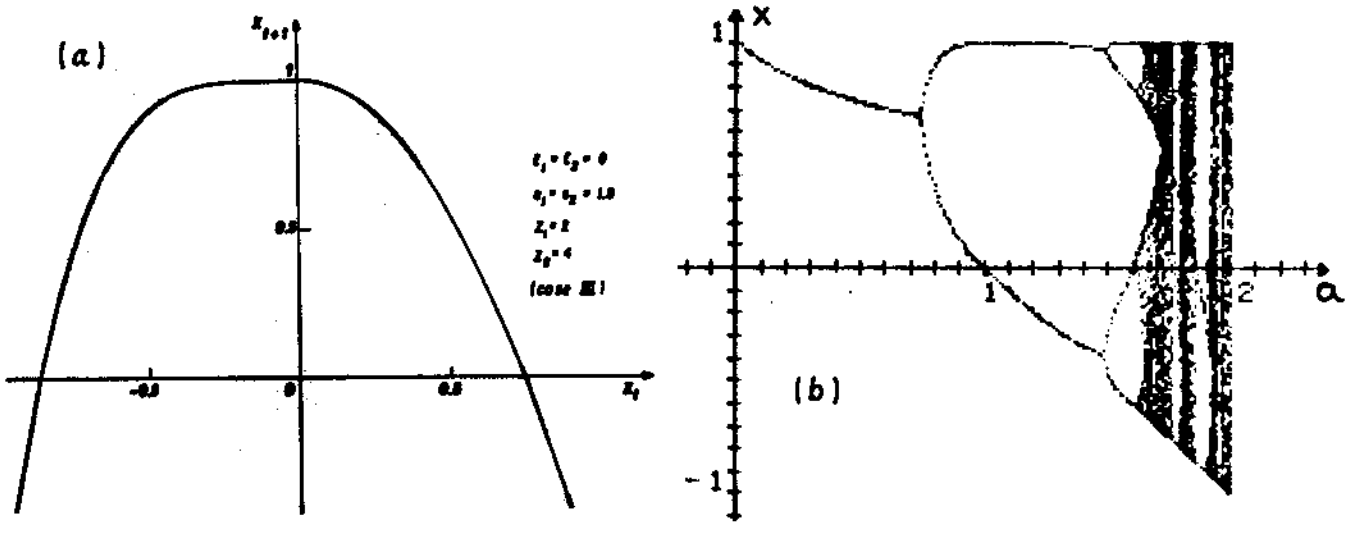

Fig. 3. (a) Asymmetric map, (b) a-evolution of the attractor and of the (c) Liapunov exponent for $(z_1,z_2)=(2,4)$, with $a_1=a_2\equiv a$ and $\epsilon_1=\epsilon_2=0$.

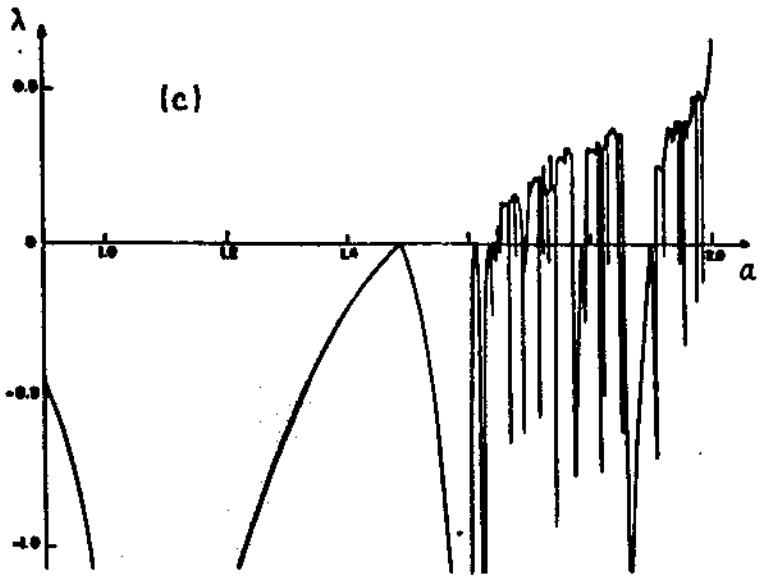

Fig. 3. continuation.

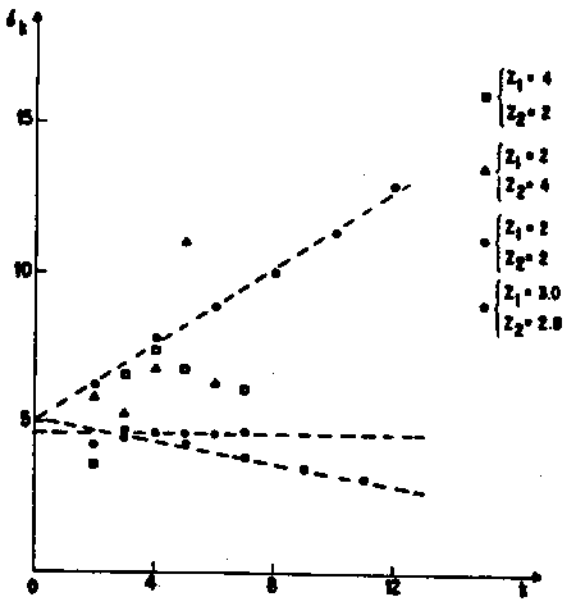

Fig. 4. Evolution of the successive ratios $\{\delta_k\}$ for the $z_1=z_2=2$ prototype and for the case II ($z_1 \neq z_2$).

4. DISCONTINUOUS MAPS (CASE III)

4.1. *Evolution of the attractor: inverse cascades*

This is the most interesting case. We observed that a new uni-

versal road to chaos is associated with this type of maps[10,14]. In Fig. 5 we have represented, for $z_1=z_2=2$ and $(\varepsilon_1,\varepsilon_2)=(0,0)$, $(0.1,0)$ and $(0,0.1)$, the dependence of a^M and a^m (values of a respectively above which and below which finite attractors disappear) as function of x_0. The Fig. 6 shows the a-dependence of the attractor for a typical case $(\varepsilon_1,\varepsilon_2)=(0,0.1)$. In this example, after a standard pitchfork bifurcation we see the appearance of sequences of inverse cascades ("inverse" refers to the fact that a must decrease in order to approach the accumulation point) in arithmetic progression, initially mixed

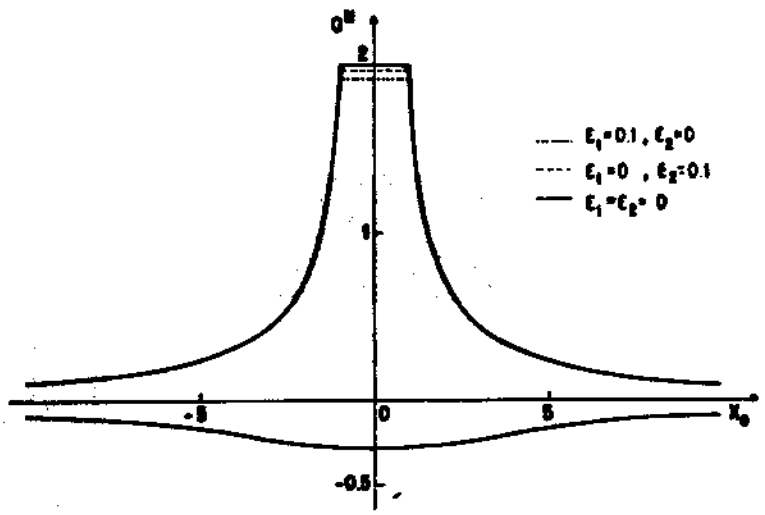

Fig. 5. Diagram of the "finite-attractor-disappearance" for $z_1=z_2=2$.

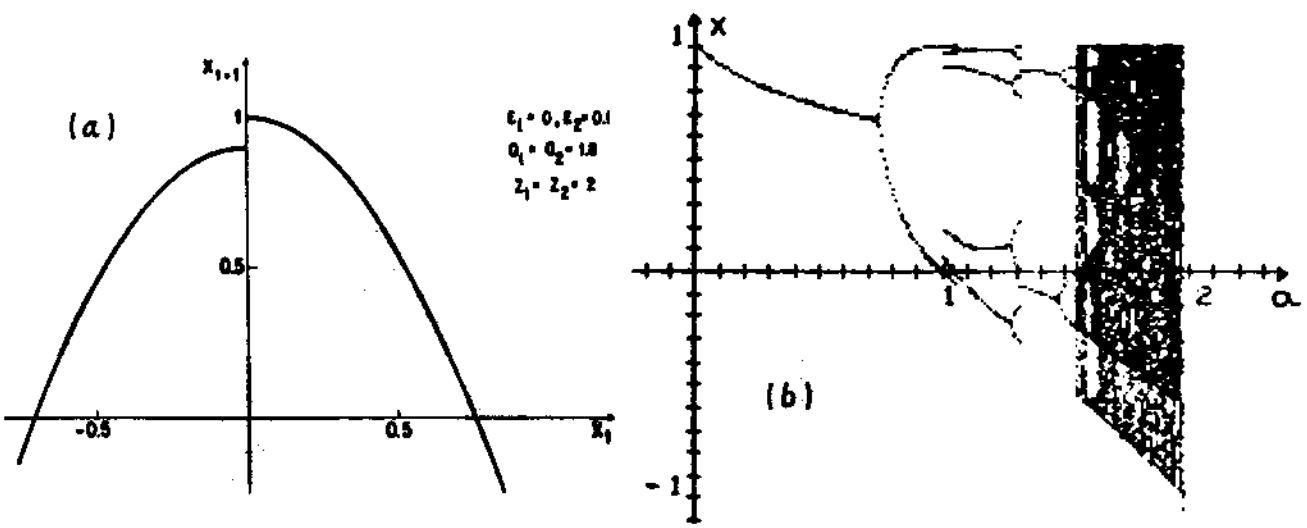

Fig. 6. (a) Discontinuous map and (b) a-evolution of the attractor for $(\varepsilon_1,\varepsilon_2)=(0,0.1)$, $z_1=z_2=2$ and $x_0=0.5$.

with pitchfork bifurcations. The first cascade is ...14→12→10 8→6→4, which accumulates on a=1. Immediately above this cascade we observe a couple of standard pitchfork bifurcations. Further on a new inverse cascade appears as follows: ...25→21→17→ 13→9 and then again a pitchfork bifurcation into period 18. Then another inverse cascade appears as follows:...76→58→40→22. After this cascade, no other standard pitchfork bifurcations are observed, but instead new inverse cascades are present: ...70→48→26, and then ...108→82→56, and then ...142→86→30, etc. A rule is observed : Within each window, the periods grow arithmetically by *adding* the first element of the previous window, namely the element immediately below its accumulation point. In fact, we have a very rich fine structure. We observe that between any two consecutive elements of a cascade there is another inverse cascade whose periods grow with the rule mentioned above. For example, between the elements 40 and 22 of the third cascade, the cascade ...102→62→22 exists. Between the elements 102 and 62 of this cascade, we have the following one ...266→164→62, and so on. The new elements of a p-furcation appears discontinuously like tangent bifurcations. However, they do not present intermittency, since the iterated function f(f(...f(x))) presents square corners which cross the x'=x bissectrix. See an example in Fig. 7. Every new element of a

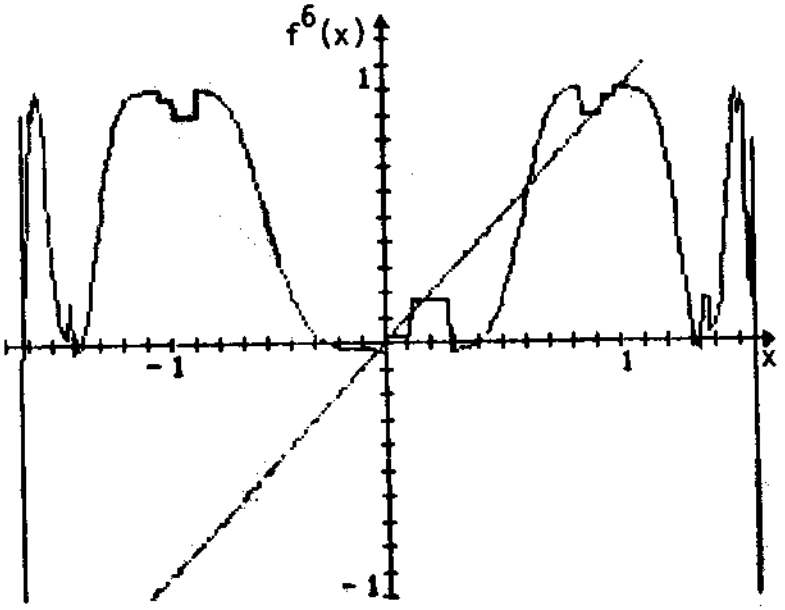

Fig. 7. Plot of $f^6(x)$ for a=1.03, $(\varepsilon_1,\varepsilon_2)=(0,0.1)$, $z_1=z_2=2$ and $x_0=0.5$.

p-furcation appears at the neighbourhood of the attractor that exists just below its accumulation point. In Fig. 8 we show an example to clarify this point. Therein, we see the cascade 18→14→10 and between the elements 14 and 10, the cascade ...38→24→10 is depicted (dashed lines).

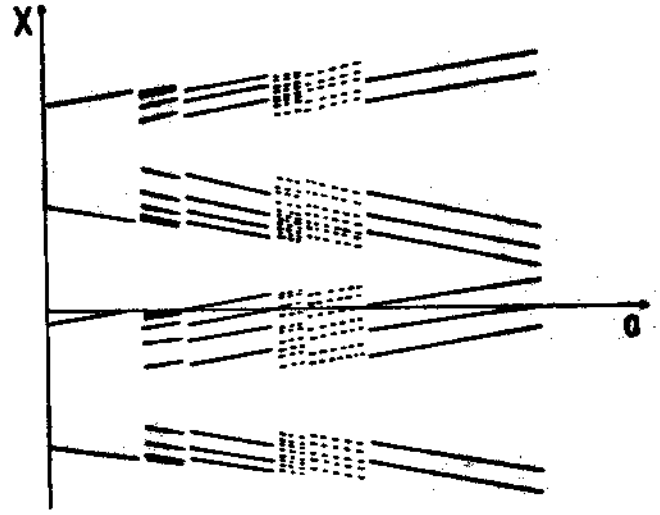

Fig. 8. Schematic example of the inverse cascade ...18→14→10 and the "intermediate" inverse cascade ...38→24→10. The figure is out of scale.

We have represented in Fig. 9 the evolution of the attractor, for a typical case, as a funtion of the size of the gap and of a. Such phase-diagram will be refered hereafter as *bunch of bananas*. Initially, let us fix ε_1 and vary a. We see the behavior described above: inverse cascades of attractors whose periods grow arithmetically and accumulate on values of a, immediately below which appear cycles whose periods precisely are the corresponding adding constants. Futhermore, between any two bananas we always have another banana. The same kind of behavior is observed by fixing a and varying ε_1 (or ε_2, or both, with $\varepsilon_1 \neq \varepsilon_2$). The accumulation points of the cascades in turn accumulate (for *increasing* a if $(\varepsilon_1, \varepsilon_2)$ are fixed) on a point *which is the entrance to chaos*. In other words, we have (presumably) an infinite number of *accumulation points where there*

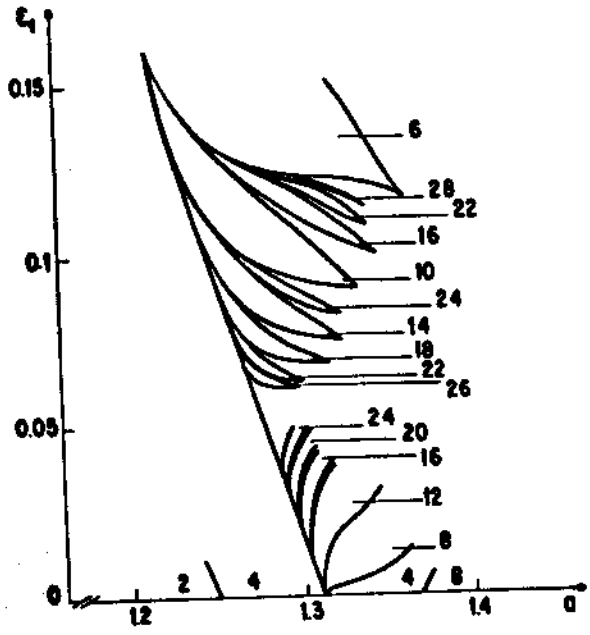

Fig. 9. Phase-diagram for $z_1=z_2=2$, $\varepsilon_2=0$ and $x_0=0.5$. The number indicates the period of the attractor. For $\varepsilon_1=0$ we recover the well known period-doubling sequence.

is no chaos (negative Liapunov exponents), as this only emerges at the accumulation point of the accumulation points.

For fixed $(\varepsilon_1,\varepsilon_2)$ a given banana exists between a minimal value a_k^m and a maximal value a_k^M. Within a given cascade of bananas (whose sequence is noted with k=1,2,3...) we verify

$$|a_k^m - a_{k+1}^m| \sim |a_{k-1}^m - a_k^m|^{z_1} \tag{5}$$

as well as

$$|a_k^m - a_\infty^m| \sim |a_{k-1}^m - a_\infty^m|^{z_1} \tag{6}$$

for k large enough. The same law holds for $\{a_k^M\}$, for all cascades, for all values of $(\varepsilon_1,\varepsilon_2)$, such that $\varepsilon_1 \neq \varepsilon_2$, in the presence or absence of higer order terms in Eq. (4), and also if we fix a and vary $(\varepsilon_1,\varepsilon_2)$.

4.2. *Length of the cycle*

For each cascade, the length of the k-th stable cycle as function of the parameter a can be determined as follows. If we denote B as the adding constant of the cascade and ξ_k the length of the k-th cycle, we have

$$\xi_k = A + Bk \tag{7}$$

where A is a natural number. Using Eq. (5), we obtain

$$\xi_k \sim \frac{B}{\ln(z_1)} \ln \ln \frac{1}{a_k - a_{k+1}} + \xi_0 \tag{8}$$

where ξ_0 is an integer number. Analogously, if we use Eq. (6) we obtain a relation identical to Eq. (8), but with $a_k - a_\infty$ replacing $a_k - a_{k+1}$. To the best of our knowledge, this is the first time such type of law is exhibited within the formalism of chaos. In Fig. 10 we show the behavior of ξ as function of a*-a for a typical case.

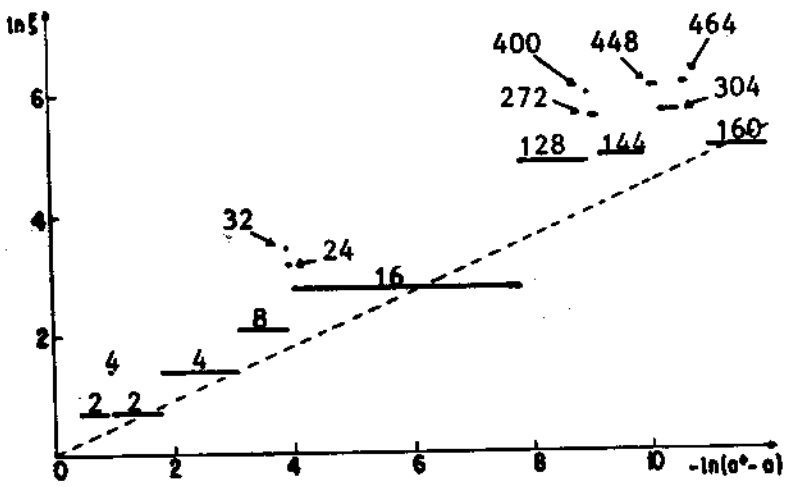

Fig. 10. Plot of ln(ξ) as function of ln(a*-a) for $(\varepsilon_1,\varepsilon_2)=(0,0.1)$, $z_1=z_2=2$ and $x_0=0.5$, and of the asymptotic behavior for the logistic case (dashed line). The numbers indicate the length of the cycle.

4.3. *Capacity dimension of the attractor at the accumulation point of a cascade*

In section 4.1 we mentioned that all new elements of a cascade appear near the elements of the attractor immediately below that cascade, on which they accumulate. If we denote $a_k^{(q)}$ the q-elements of the k-th attractor of a given cascade ($q<\xi_k$; increasing q denotes approach to the accumulation point), the following laws are observed

$$|x_k^{(q)} - x_k^{(q+1)}| \sim |x_k^{(q-1)} - x_k^{(q)}|^{z_1} \tag{9}$$

or equivalently

$$|x_k^{(q)} - x_k^{(\infty)}| \sim |x_k^{(q-1)} - x_k^{(\infty)}|^{z_1} \tag{10}$$

for q and k large enough. These laws enable us to calculate the capacity dimension of the attractor at the accumulation point of any cascade. The capacity dimension of a set is defined as

$$d_c = \lim_{\varepsilon \to 0} \frac{\ln N(\varepsilon)}{\ln (1/\varepsilon)} \tag{11}$$

where $N(\varepsilon)$ is the minimal number of segments (for unidimensional cases) needed to cover the set. If we adopt $\varepsilon \equiv |x_k^{(1)} - x_k^{(2)}|^{z_1}$, then $N(\varepsilon)=q$, hence $d_c=0$. In contrast, for continuous symmetric maps the capacity dimension of the attractor at the accumulation point of the cascades is a non integer number, between 0 and 1, for finite z (e.g., for $z=2$, $d_c \cong 0.537$). To avoid confusion, it is worthy to recall here that chaos within the gap road only appears at the accumulation point of the accumulation points; at the entrance of chaos non trivial dimensionalities are exhibited as discussed in section 4.7

4.4. *Crossover to the period-doubling scenario*

The number of pitchfork bifurcations in the discontinuous maps is a function of the size of the gap. It increases when the

size of the gap decreases. For example, for $(\varepsilon_1,\varepsilon_2)=(0,0.0001)$ we observe *six* pitchfork bifurcations (mixtured with inverse cascades), whereas for $(\varepsilon_1,\varepsilon_2)=(0,0.1)$ there are only *three* pitchfork bifurcations. In the a-evolution of the attractor a cycle which results from a pitchfork bifurcation can reappear further on: See cycle of size two in Fig. 10. This cycle disappears at the value $a_d=(1-\varepsilon_1)^{1-z_1}$ and at $a_r=(1-\varepsilon_1)/(1-\varepsilon_2)^{z_1}$ it reappears. To be more precise, these values are slighty modified according to the attractor towards which the sistem evolves, which in turn depends on the initial value x_0, as discussed in section 4.6. The reappearance of the cycle with period two can even happen above the first entrance into chaos. For example, the map with $(\varepsilon_1,\varepsilon_2)=(-0.1,0.1)$ first enters into chaos at $a^*\cong 1.23$, whereas $a_r\cong 1.358$. Notice that for $\varepsilon_1=\varepsilon_2\equiv\varepsilon$ (continuous map), we have $a_d=a_r=(1-\varepsilon_1)^{1-z_1}$, a fact which clearly illustrate how the crossover to the period-doubling scenario occurs. A similar study can be made for cycles with period 4,8, etc.

4.5. *Liapunov exponent*

In Fig. 11 we present the a-evolution of the Liapunov exponent for a typical case $(\varepsilon_1,\varepsilon_2)=(0,0.1)$. The first entrance into chaos in this case occurs at $a^*\cong 1.5447414$. We see in Fig. 11(c), which is an amplification of Fig. 11(b), remarkable features: (i) the stucture is roughly self-similar, (ii) the "fingers" corresponding to high periods are very narrow. For a given cascade they monotonously become narrower and shift towards negative values of λ, thus exhibiting (presumably) *infinitely large periods with no chaos*. The highest and largest finger of each cascade corresponds to the lowest period of that cascade; if we consider increasingly large lowest periods, the tops of the fingers approach $\lambda=0$, and drive the systems into chaos, (iii) changements of periods occur for $\lambda\to^{-}-\infty$, in remarkable contrast with changements of periods in the period-doubling road, which occur at $\lambda=0$.

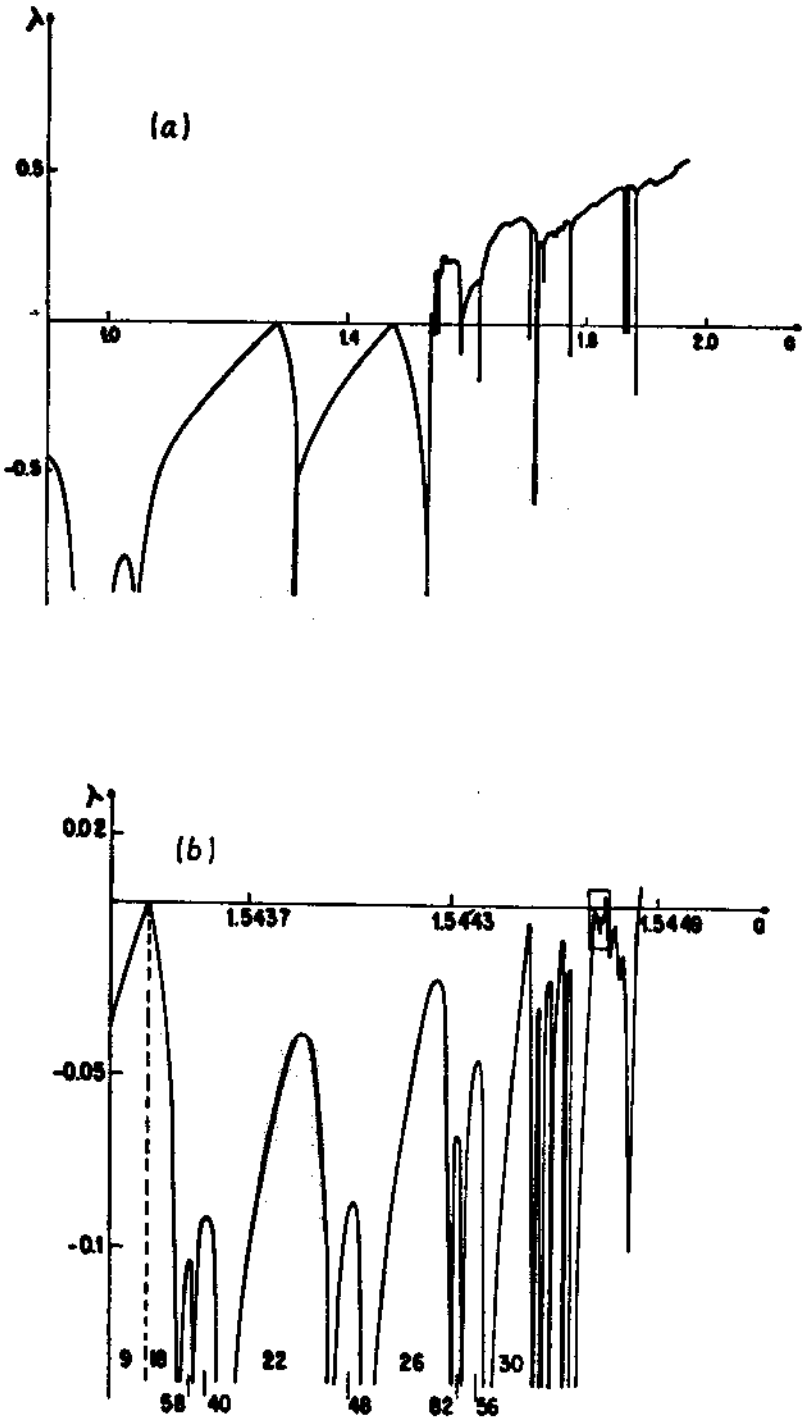

Fig. 11. Evolution of the Liapunov exponent as function of a for $(\varepsilon_1,\varepsilon_2)=(0,0.1)$, $z_1=z_2=2$ and $x_0=0.5$. The numbers in the fingers indicate the period of the attractor (c) is the amplification of the small rectangle in (b).

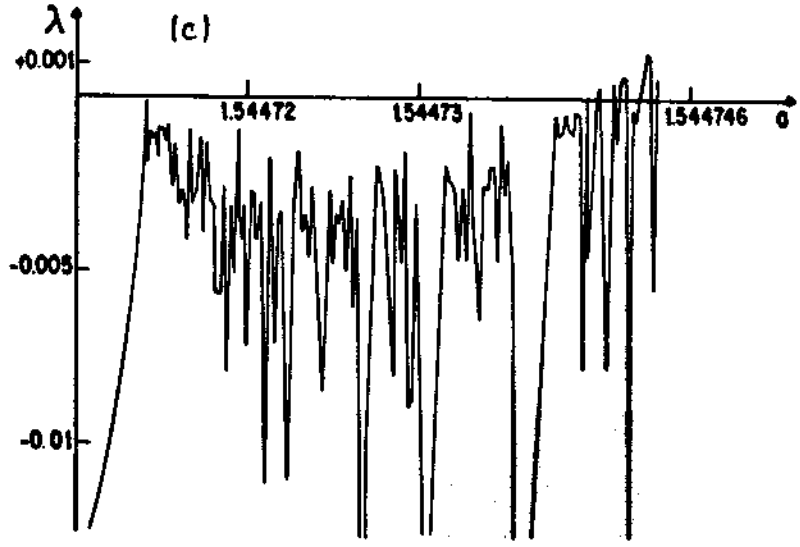

Fig. 11. continuation.

4.6. *Uncertainty exponent*

Continuous one-dimensional maps presenting an unique extremum have at most one finite attractor, which is independent on the initial condition. In maps with a gap at the extremum we verify that this picture is modified. In such cases, more than one finite attractor (typically two attractors) appear when we cross from one banana (see Fig. 9) to a neighbouring one (we observed this in several crossings, it might happen in all of them). The attractor which is chosen depends on the initial value x_0. Two examples are presented in Fig. 12(a) for a=1.3 (a=1.540344); the black and white regions are euclidean (dimensionality D=1) where as the border-set between them is a fractal with capacity dimension d. The uncertainty exponent[15] α_u is given by α_u=D-d. The system is said to present *final-state* sensitivity or non-sensitivity according be $0\leq\alpha_u<1$ or $\alpha_u=1$. To calculate α_u we consider, in the interval of x_0 corresponding to finite attractor(roughly [-1,1]), N randomly chosen values (typically $N=10^4$). We then choose ε (say 10^{-3} and below) and check whether both attractors starting from $x_0\pm\varepsilon$ coincide with that of x_0; if not, that value of x_0 is said *uncertainty*. We note N_u the total number

of uncertainty points. The uncertainty ratio N_u/N varies as ε^{α_u}. We find $\alpha_u \simeq 0.85$ ($\alpha_u \simeq 0.22$) for a=1.3 (a=1.540344).

Numerical experiments based on forth and back variations of a might present hysteresis according to the initial value x_0 retained for the various steps. In Fig. 12(b) we exhibit a cycle of hysteresis. The system is "prepared" initially with $x_0=0$ and a=1.3, which drives the system to a cycle with period two. Futher on, after some iterations the control parameter a is tuned to a=1.2 with an initial condition x=0.8971, then the limiting cycle now has period four. After some iterations the system is brought back to a=1.3 with an initial condition a=-0.1703. We observe that the period in this situation is not any more two, but eight. This hysteresis phenomenon can help the experimental identification of the gap road to chaos.

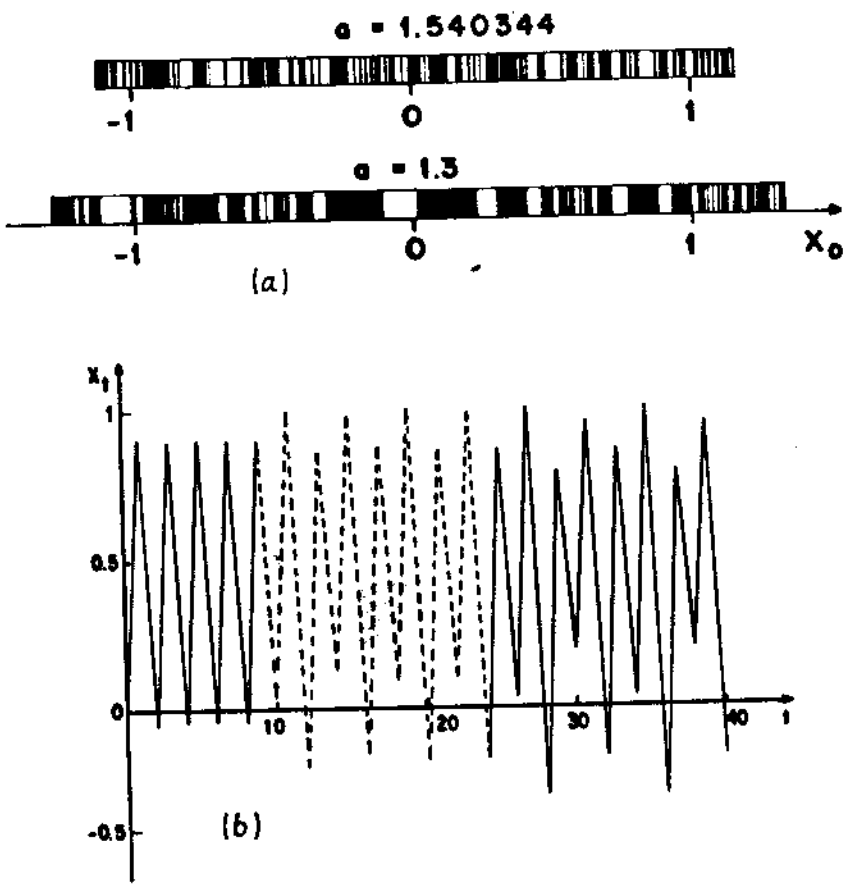

Fig. 12. (a) Basins of attraction and (b) hysteresis cycle for typical values of a and $(\varepsilon_1,\varepsilon_2)=(0,0.1)$ and $z_1=z_2=2$. In (a), for a=1.3(a=1.540344) the black and white regions correspond to cycles with period 8 and 2 (25 and 21).

4.7. *Multifractality*

The attractor at the accumulation point of the bifurcations governed by Eq.(1) is a complicated object. The probability of distribution of its points is non uniform, a reason for which this object is called a *multifractal*[16]. The formalism used to study multifractals consists in covering the attractor with boxes, indexed by i, of size l_i and assume that the probability density scales like $p_i \propto l_i^{\alpha}$, in the limit $l_i \to 0$. The characterization of a multifractal is through the function $f(\alpha)$, which is the dimension of the set of boxes which share a given index α. Through a Legendre transformation, $f(\alpha)$ is related to the generalized dimensions D_q[17]. The minimal and maximal values of α respectively coincide with D_∞ and $D_{-\infty}$; the maximal value of $f(\alpha)$ coincides with the Hausdorff dimension D_0. The attractor of the *discontinuous* map at the first entrance into chaos also is a multifractal. In Fig. (13) we present $f(\alpha)$ for the case $(\varepsilon_1,\varepsilon_2)=(0,0.1)$. Its shape is different (more square-like) from that obtained without gap (period-doubling road to chaos), and the values we obtain are $D_0 \cong 0.95$, $D_\infty \cong 0.45$ and $D_{-\infty} \cong 5.7$.

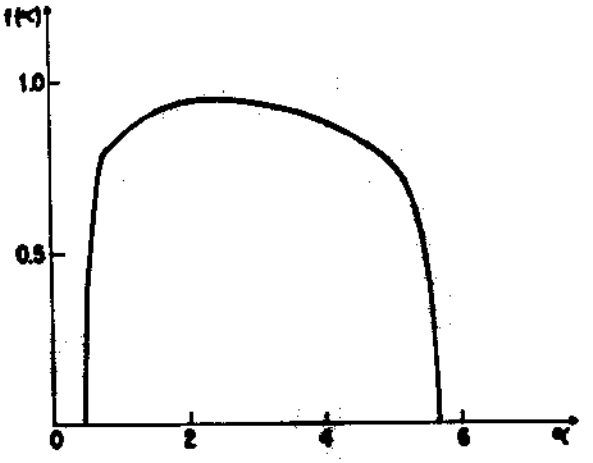

Fig. 13. Multifractal function $f(\alpha)$ for $(\varepsilon_1,\varepsilon_2)=(0,0.1)$, $z_1=z_2=2$ and $x_0=0.5$ (chaos appears at $a^* \cong 1.5447414$).

5. CONCLUSIONS

We have verified that the period-doubling scenario for one-dimensional one-extremum maps is strongly modified if an asymmetry is introduced at the extremum. Amplitude asymmetry ($a_1 \neq a_2$) and exponent asymmetry ($z_1 \neq z_2$) do not alter the bifurcation sequence, but introduces remarkable numerical differences while approaching the first entrance to chaos. The unique tendency associated with the set $\{\delta_k\}$ disappears. By far, the more interesting case occurs for discontinuous maps ($\varepsilon_1 \neq \varepsilon_2$). Sequences of inverse cascades in arithmetic progression are observed in the evolution of the attractor. There is no chaos at the accumulation point of these cascades, which appears only at the accumulation point of the accumulation points. Several other unusual fatures were found at the phase-diagram, Liapunov and uncertainty exponents, multifractality, among others. This behavior presents universality and can be considered as a new road to chaos.

We acknowledge with pleasure very fruitful suggestions by H.W. Capel, M. Napiórkowski, as well as interesting remarks by A. Coniglio, E.M.F. Curado , H.J. Herrmann, B.A. Huberman and J.P. van der Weele. We are indebted to P. Coullet and C. Tresser for calling our attention on Ref. 7.

REFERENCES

1. R.M. May, Nature 261, 459 (1976).
2. A. Libchaber, C. Laroche and S. Fauve, J. Phys. Lett. 43, L211 (1982).
3. J.L. Hudson and J:C. Mankin, J. Chem. Phys. 74, 6171 (1981).
4. F.T. Arecchi, R. Meucci, G. Puccioni and J. Tredicce, Phys. Rev. Lett. 49, 1217 (1982)
5. S. Grossmann and S. Thomae, Z. Naturf. 32A, 1353 (1977); M. J. Feigenbaum, J. Stat. Phys. 21, 669 (1979); P. Coullet and C. Tresser, J. Phys. (Paris) Colloq. 5, C25 (1978).
6. M. Metropolis, M.L. Stein and P.R. Stein, J. Combinatorial Theory (A) 15, 25 (1973).
7. Arneodo, P. Coullet and C. Tresser, Phys. Lett. 70A, 74 (1979).
8. P. Szepfalusy and T. Tél, Physica 16D, 252 (1985); J.M.Gambaudo, I. Procaccia, S. Thomae and C. Tresser, Phys. Rev. Lett. 57, 925 (1986).
9. R.V. Jensen and L.K.H. Ma, Phys. Rev. A 31, 3993 (1985).
10. M.C. de Sousa Vieira, E. Lazo and C. Tsallis, Phys. Rev. A 35, 945 (1987).
11. A.A. Hnilo, Optics Commun. 53, 194 (1985); A.A. Hnilo and M.C. de Sousa Vieira, to appear in J. Opt. Soc. Am.
12. M. Octavio, A. Da Costa, and J. Aponte, Phys. Rev. A 34, 1512 (1986).
13. P.R. Hauser, C. Tsallis and E.M.F. Curado, Phys. Rev. A 30, 2074 (1984); J.P. Eckmann and P. Wittwer, Computer Methods and Borel Summability Applied to Feigenbaum's Equation, Lectures Notes in Physics, vol. 227 (Springer, Berlin, 1985); J.P. van der Weele, H.W. Capel and R. Kluiving, Phys. Lett. 119A, 15 (1986); J.K. Bhattacharjee and K. Banerjee, J. Phys. A 20, L269(1987).
14. M.C. de Sousa Vieira and C. Tsallis, to be published.
15. C. Grebogi, S.W. McDonald, E. Ott and J.A. Yorke, Phys. Lett. 99A, 415 (1983); M. Napiorkowski, Phys. Lett. 113A, 111 (1985).

16. T.C. Halsey, M.H. Jensen, L.P. Kadanoff, I. Procaccia, and B.I. Shraiman, Phys. Rev. A 33, 1141 (1986).
17. H.G.E. Hentschel and I. Procaccia, Physica 8D, 435 (1983).